Planet migration in self-gravitating protoplanetary discs

ISIMA final report - 12th August 2010

Farzana Meru[1] & Clement Baruteau[2]

[1]University of Exeter, UK
[2]University of California, Santa Cruz, USA

Abstract

We carry out two-dimensional hydrodynamical simulations to investigate the effects of the turbulence caused by gravitational instability on the migration of a 10 Jupiter-mass planet. We model three discs with different amounts of turbulence and model two scenarios: the first scenario allows the planet to migrate immediately and we find that the migration rates are similar in all three discs, regardless of the amount of turbulence. The second method involves keeping the planet fixed on a circular orbit such that it opens up a gap, before allowing it to migrate. We find that though the gap properties appear to be similar in all three cases, the migration rate is faster in a disc with a lower amount of turbulence.

1 Introduction

Over the last two decades, observers have detected a large number of extra-solar planets with extremely diverse properties. Figure 1 shows a plot of the mass of all the extra-solar planets against their semi-major axis that have been discovered by the various techniques. It is very evident that the properties differ greatly from those planets in our own solar system. The majority of extra-solar planets have been discovered by the *radial velocity* and *transiting* techniques which typically detect planets close to the central star. Advances in the *adaptive optics* technique has meant that recent times have seen the birth of planet detection by *direct imaging*. Since direct imaging requires a high brightness contrast between the planet and parent star, the planets have been observed at large radii ($\gtrsim$ O(10) AU, Kalas et al. 2008; Marois et al. 2008; Lagrange et al. 2010; Lafrenière et al. 2010). One such example is the HR 8799 system (Marois et al. 2008) which was the first directly imaged multi-planet system. This system consists of three planets with estimated masses of 7, 10 and 10M_J at projected separations of 24, 38 and 68 AU, respectively.

Some of the key questions that need to be answered about such a diverse range in planets is how did they form, how have they grown, what was their evolutionary process, and how have they ended up in the locations in which we observe them today. The standard core accretion scenario (Safronov 1969; Goldreich & Ward 1973; Perri & Cameron 1974; Harris 1978; Mizuno 1980), involving the coagulation of the dust components of the protoplanetary disc into larger bodies which may remain as terrestial planets or accrete a gaseous envelope to form giant

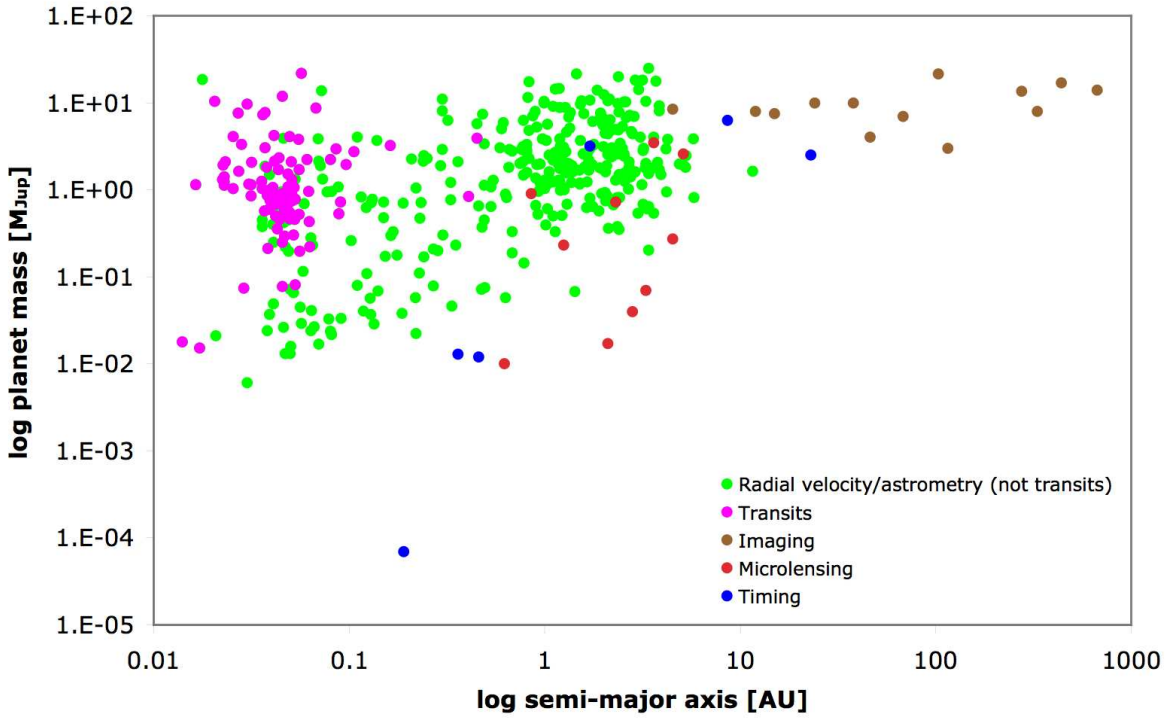

Figure 1: Graph of the mass against semi-major axes of all the extra-solar planets discovered, separated out by the detection technique. Data taken from exoplanet.eu.

planets, has been able to describe the formation of planets close to the central star ($\lesssim 5$ AU). However, this mechanism is unable to form planets at large radii, though secondary mechanisms such as scattering or outward planetary migration may offer a potential other solution to this.

The second in-situ planet formation scenario is gravitational instability (Kuiper 1951; Cameron 1978; Boss 1997). This mechanism is typically thought to operate further from the central star (Rafikov 2005; Matzner & Levin 2005). This scenario involves early-stage protoplanetary discs which are massive enough for its self-gravity to play a part in its evolution. Such discs have characteristic spiral structures which have been observed in real discs in the past (e.g. Grady et al. 2001; Fukagawa et al. 2004). Future telescopes such as the Atacama Large Millimetre Array (ALMA) are expected to be able to see such spiral structures in the millimetre waveband, with much higher precision than before.

Gravitationally unstable discs are subject to pressure and rotational forces which stabilise the disc on small and large scales, respectively, while gravity acts to destabilise the disc. If the latter force overcomes the former two, the disc may fragment. If the disc does not fragment, it may still be subject to turbulence caused by the gravitational instability. The stability of a self-gravitating disc can be described by the stability parameter (Toomre 1964):

$$Q = \frac{c_{\rm s}\kappa_{\rm ep}}{\pi\Sigma G}, \tag{1}$$

where $c_{\rm s}$ is the sound speed in the disc, $\kappa_{\rm ep}$ is the epicyclic frequency, which for Keplerian discs is approximately equal to the angular frequency, Ω, Σ is the surface mass density and G is the gravitational constant. Toomre (1964) showed that for an infinitesimally thin disc to fragment, the stability parameter must be less than a critical value, $Q_{\rm crit} \approx 1$. However, for the turbulence

due to the disc self-gravity to be important, $Q \lesssim 2$.

In addition to the Toomre stability parameter, the cooling rate in a disc is also important. For a steady-state disc with no external heating, the cooling in the disc balances the heating due to the disc self-gravity. If a disc is allowed to cool, the gravitational instability will become stronger (since the ratio of the gravitational to the pressure forces will increase). This will cause the spiral structures to form resulting in compressive, shocked regions which will then heat up the disc. As the disc heats up, the gravitational instability becomes less prominent and the heating due to it reduces. The disc then starts to cool more than it is heated and the cycle repeats causing the disc to maintain a steady state. However, Gammie (2001) showed that if the cooling timescale can be parameterised as

$$\beta = t_{\rm cool}\Omega, \tag{2}$$

where

$$t_{\rm cool} = u\left(\frac{du_{\rm cool}}{dt}\right)^{-1}, \tag{3}$$

u is the internal energy and $du_{\rm cool}/dt$ is the total cooling rate, then for fragmentation we require $\beta \lesssim \beta_{\rm crit}$, where $\beta_{\rm crit}$ is a critical value of the cooling timescale in units of the orbital timescale. Rice, Lodato, & Armitage (2005) carried out three-dimensional simulations using a Smoothed Particle Hydrodynamics (SPH) code and showed that this cooling parameter is dependent on the equation of state while more recently, Meru & Bate (2010) showed that the critical value of the cooling parameter is dependent on the disc and star conditions.

Gammie (2001) also showed that in a steady-state α-disc, the cooling timescale in units of the orbital timescale, β, can be related to the gravitational stress,

$$\alpha_{\rm GI} = \frac{4}{9}\frac{1}{\gamma(\gamma-1)}\frac{1}{\beta}, \tag{4}$$

where γ is the ratio of specific heats.

Many previous simulations of self-gravitating discs consider the fragmentation of these discs into bound objects, but due to computational difficulty, the evolution of these objects have not been considered in too much detail. In particular, an important question to answer is how the planets that may form via the disc instability method interact with the disc and in particular, how are they affected by the background turbulence caused by the disc self-gravity. In addition, do such planets migrate in the disc as they have been shown to do in simulations that do not employ strong self-gravity? Does the self-gravitating turbulence stop large mass planets from opening up a gap, which they would be expected to do? How do the disc and planet interact and what is the net torque induced on the planet? In addition, does the planet migrate and in what direction?

This project begins to answer these questions by way of carrying out two-dimensional hydrodynamical simulations. In Sections 2 and 3, we describe the numerical method and simulations being carried out to explore this topic, respectively. In Section 4 we carry out some consistency checks with previous work. In Section 5, we present some preliminary results and finally in Section 6, we present our preliminary thoughts and future directions.

2 Numerical method

The simulations presented here have been carried out using FARGO, a two-dimensional grid based hydrodynamics code (Masset 2000; Baruteau & Masset 2008a,b). The code includes the

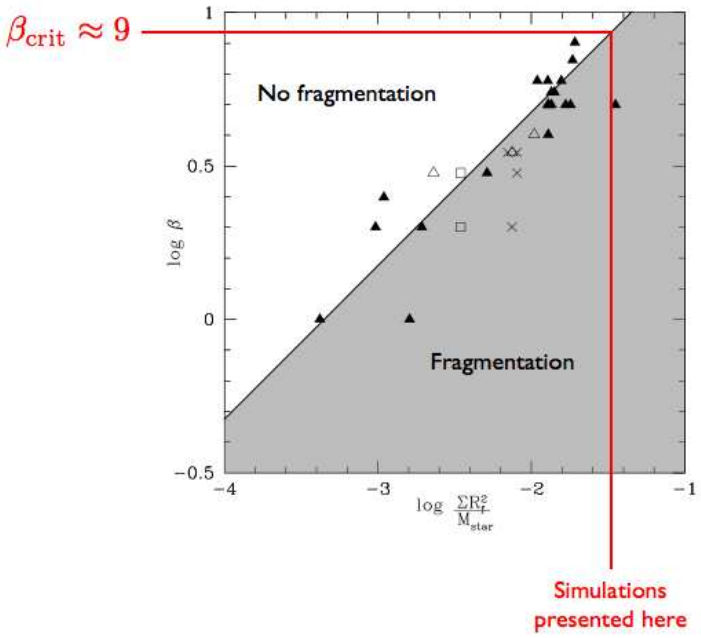

Figure 2: Graph of the cooling timescale in units of the orbital timescale, β, against $\Sigma R^2/M_\star$ from Meru & Bate (2010). The solid line shows the critical value below which fragmentation will occur. For the simulations presented here, the critical value according to Meru & Bate (2010) is expected to be, $\beta_{\rm crit} \approx 9$.

heating due to gravitational instabilities and the cooling using the parameterisation given by equation 2, detailed in Section 3. The simulations presented are carried out using a resolution of 256 and 768 cells in the radial and azimuthal directions, respectively. The cells in the azimuthal direction are equally spaced whereas a logarithmic spacing is used in the radial direction such that the inner regions are better resolved than the outer regions. We use an open boundary at both the inner and outer radii of the discs.

3 Simulations

We simulate a $0.2{\rm M}_\odot$ disc around a $1{\rm M}_\odot$ star (modelled using a potential), spanning $20 \leq R \leq 250$ AU. The initial surface mass density and temperature profiles are $\Sigma \propto R^{-1}$ and $T \propto R^{-1/2}$, respectively. The magnitudes of these are set such that the Toomre stability parameter at the outer edge of the disc, $Q_{\rm min} = 2$. The discs that are initially laminar are evolved without a planet to allow the discs to achieve a self-gravitating state using values of the cooling timescale in units of the orbital timescale, $\beta = 5$, 15, 20 and 30. Equation 4 shows that the gravitational stress in the disc, $\alpha_{\rm GI}$, is directly related to the cooling timescale in units of the orbital timescale, β, such that a faster cooling results in stronger gravitational stress. Therefore, by varying β, we investigate the effects of different levels of turbulence.

We then introduce a $10{\rm M}_{\rm J}$ planet at $R = 100$ AU in all the discs except the disc with $\beta = 5$. The planet is modelled using a potential with a softening, $\epsilon = 0.3H$, where H is the isothermal scaleheight in the disc given by $H = c_{\rm s}/\Omega$. The planet is introduced over 10 orbits by increasing its mass linearly over time, to avoid a violent initialization for the disc. We simulate the migration of the planet in two ways: firstly, we allow the planet to migrate immediately. Secondly, since we expect that such a large planet would open up a gap, we keep the planet fixed on a circular orbit for 50 orbits (at the planet's location), to give it the opportunity to open up a gap, before allowing it to migrate.

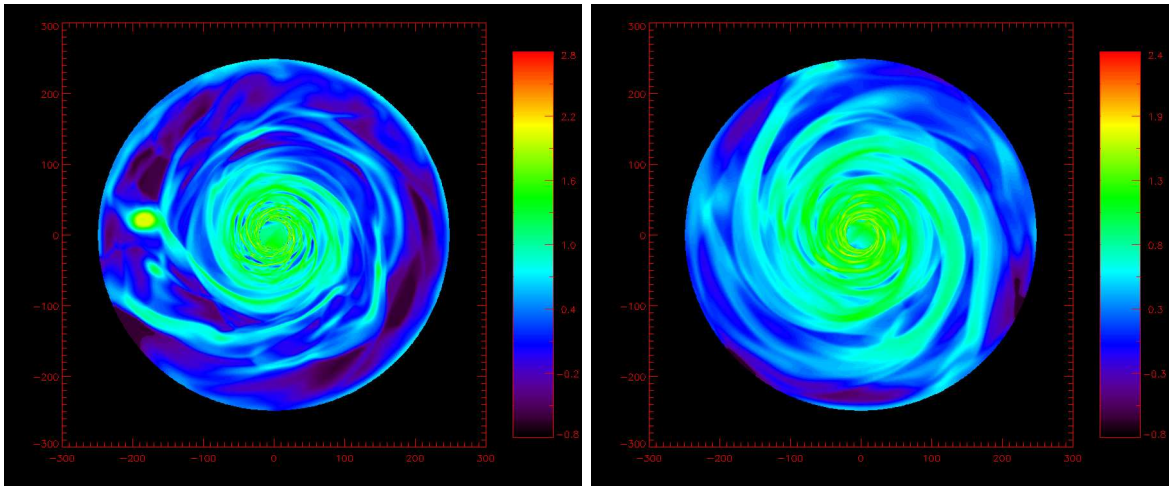

Figure 3: Surface mass density of the $0.2M_{\odot}$ disc modelled with a cooling timescale of $\beta = 5$ (left panel) and $\beta = 15$ (right panel). The fragmentation seen in the simulation with a faster cooling is consistent with the results of Meru & Bate (2010).

4 Consistency checks with previous studies

To ensure that the discs are set up correctly, we compare them to previous work. Firstly, since the aim is to understand migration of a single planet in a turbulent environment caused by gravitational instability, it is important to ensure that the disc is sufficiently gravitationally unstable, but that fragments do not form in the disc. According to Meru & Bate (2010), the disc and star setup presented here requires that for fragmentation to occur, the cooling timescale (in units of the orbital timescale), $\beta \lesssim 9$ (Figure 2). Figure 3 shows images of the disc modelled with $\beta = 5$ and 15 (left and right panels, respectively). It can be seen that with a faster cooling than the critical value determined from Meru & Bate (2010), the disc fragments whereas a slower cooling does not, and is therefore consistent with previous work.

Previous work shows that for a gravitationally unstable disc that does not fragment, the disc will settle so that the Toomre stability parameter, $Q \approx 1$ for most of the disc (e.g. Gammie 2001; Rice et al. 2005; Lodato & Rice 2004; Meru & Bate 2010). Figure 4 (left panel) shows the azimuthally averaged Toomre stability profile for these discs and shows that the disc does settle to a constant value over most of the disc. In addition, previous studies of global disc simulations show that for low mass discs, the surface mass density profile does not change significantly as the simulation progresses. We find that this is indeed the case here whereby over most of the disc, the surface mass density is similar to the initial disc setup (Figure 4; right panel).

Lodato & Rice (2004) carry out simulations of self-gravitating discs and show that there are two contributions to the stress. Firstly, the disc self-gravity causes a gravitational stress in the discs as described by equation 4. Secondly, the density perturbations as a result of the gravitational instability also causes a Reynolds stress. Figure 5 shows the azimuthally averaged values of the gravitational and Reynolds stresses averaged over 20 orbits (at 100 AU) and shows that the gravitational stress is larger than the Reynolds stress, in agreement with the simulations by Lodato & Rice (2004) and also in agreement with the analytical estimate given by Gammie (2001, equation 4).

Lodato & Rice (2004, 2005) also show that for higher disc masses ($\gtrsim 0.3M_{\odot}$), the structure becomes more dominated by low order modes i.e. high mass discs show fewer more extended spiral arms. For the simulations of low mass discs presented in this project, it is expected that a dominant mode does not exist. We therefore compute the first Fourier components of the

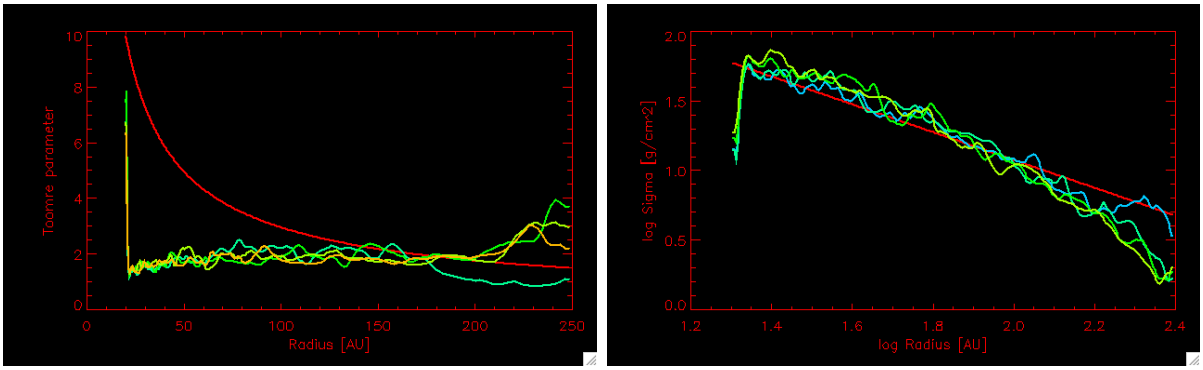

Figure 4: Toomre stability (left panel) and surface mass density (right panel) profile of the disc simulation with cooling timescale, $\beta = 15$, at the start of the simulation (red line) and every 10 orbits at 100 AU. The Toomre stability profile settles to roughly a constant value. The surface mass density profile does not change significantly as the simulation progresses. This is as expected from previous numerical simulations of self-gravitating discs.

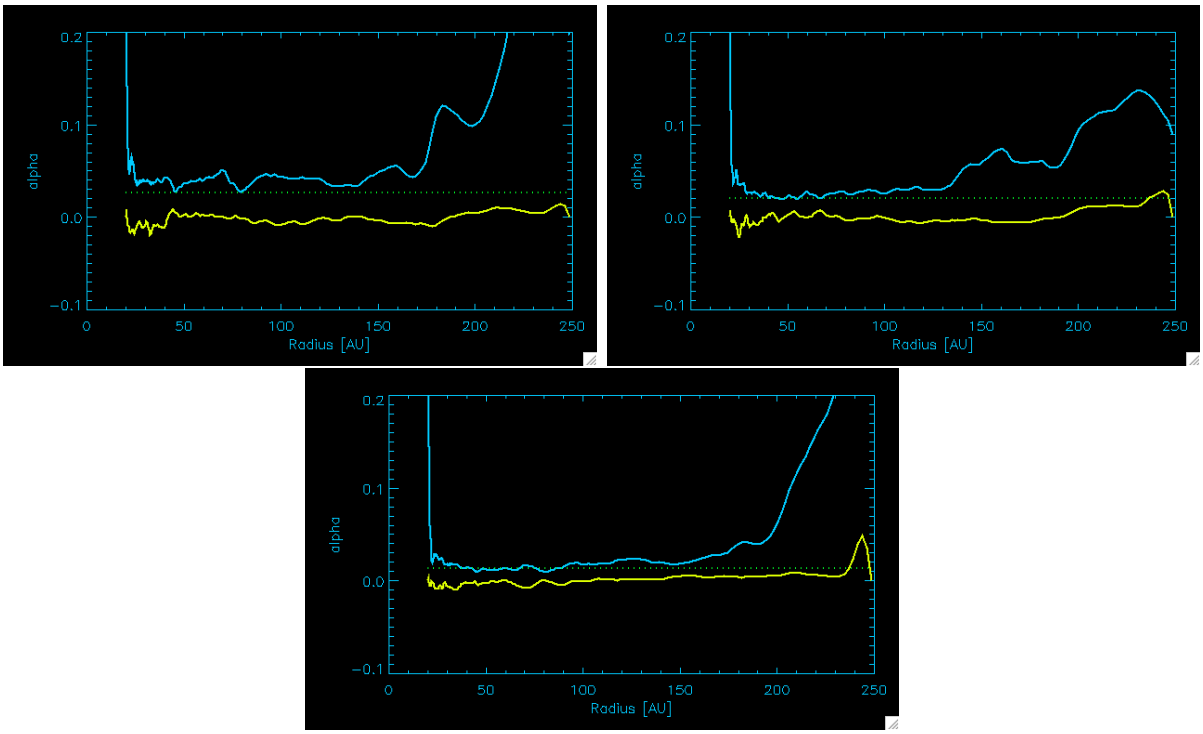

Figure 5: Graphs of gravitational stress (cyan line) and the Reynolds stress (yellow line) against radius, averaged over 20 orbits at 100 AU, for the discs modelled with a cooling timescale, $\beta = 30$ (top left panel), 20 (top right panel) and 10 (bottom panel). The dotted lines show the expected value of the gravitational stress for each simulation, determined using equation 4. The gravitational stress dominates over the Reynolds stress (in agreement with Lodato & Rice 2004) and is in reasonable agreement with that expected from the analytical expression.

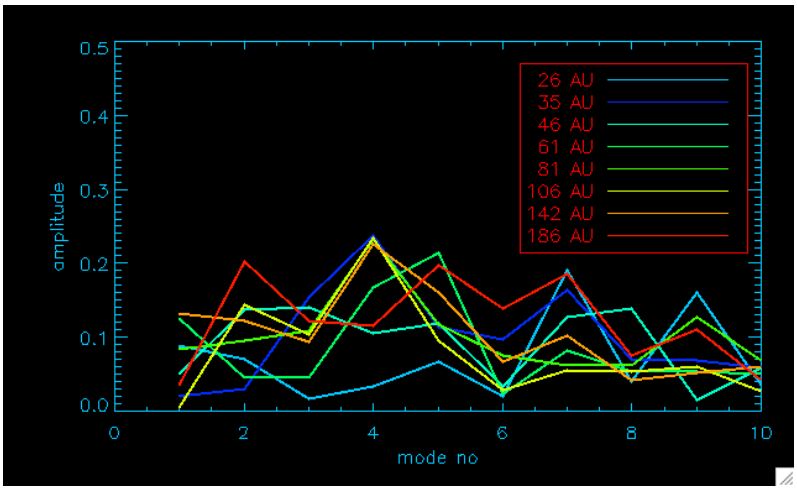

Figure 6: Graph of the first fourier component of the disc modelled with a cooling timescale, $\beta = 15$, for a number of different radii. A dominant mode does not exist, a result consistent with previous simulations of low mass discs (Lodato & Rice 2004).

density structure for a number of radii (Figure 6) and show that these discs do not have a dominant mode, as expected from previous results.

The results presented here show that the disc simulations are consistent with previous results.

5 Preliminary results

We introduce the planet (modelled using a Plummer potential with softening length, $\varepsilon = 0.3H$) in the self-gravitating disc at a radius of 100 AU over 10 orbits (at 100 AU). We carry out two sets of simulations: firstly, we allow the planet to migrate immediately (while being introduced into the disc), and secondly, we fix the planet on a circular orbit for 50 orbits to allow it to open up a gap that is roughly in steady-state, before allowing it to migrate.

5.1 Allow the planet to migrate immediately

Figure 7 shows the evolution of the planet's semi-major axis for each of the simulations with cooling timescales, $\beta = 15$, 20 and 30. Though the exact time at which the planet migrates differs slightly between the simulations, it can be seen that the migration rate is similar in all three cases, regardless of the strength of the gravitational stress. Since we allow this planet to migrate immedtaely, it does not have the chance to open up a gap. We therefore expect that the timescale on which the planet migrates is the Type I migration timescale, given by

$$t_{\rm mig,I} \approx \frac{h^2 M_\star}{4\pi C_I q \Sigma_p a^2} t_{\rm orb} \tag{5}$$

where h is the aspect ratio in the disc, $M_\star$ is the mass of the central star, $\Sigma_{\rm p}$ is the surface mass density in the disc at the planet's location, q is the planet to primary star mass ratio, a is the semi-major axis, $t_{\rm orb}$ is the orbital timescale at the planet's location and $C_{\rm I}$ is a constant which can be shown to have a value, $C_{\rm I} = {\rm O}(1)$. An order of magnitude calculation shows that the type I migration timescale is approximately a few orbits (at the planet's location) which is equivalent to $\approx {\rm O}(10^3)$ years. We indeed see that the planet does migrate to the inner edge of the disc within this time.

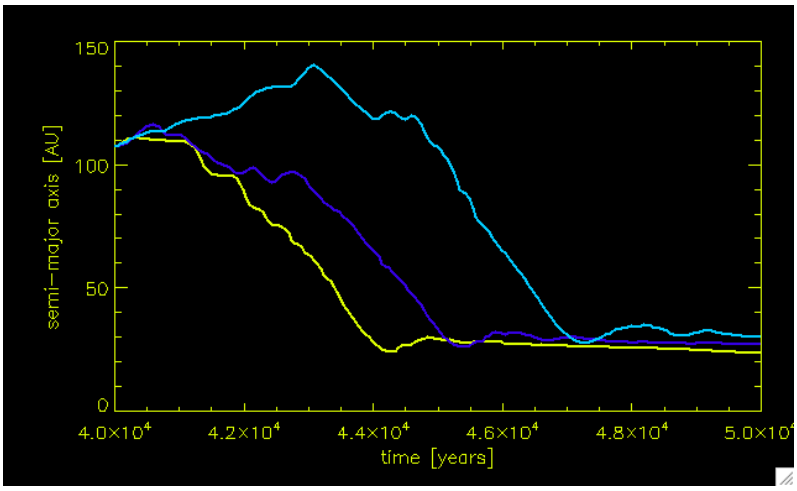

Figure 7: Plot of semi-major axis over time for the simulations which allow the planet to migrate immediately. The migration rates for the discs with cooling timescales, $\beta = 15$ (yellow line), 20 (blue line) and 30 (cyan line) are reasonably similar.

5.2 Allow the planet to open up a gap

When a planet is embedded in a disc, angular momentum exchanges occur firstly between the planet and the fluid elements located at the Lindblad resonances (Goldreich & Tremaine 1979), and secondly, between the planet and the fluid elements that corotate with the planet (Ward 1991). These are termed the Lindblad and corotation torques, respectively. If a planet opens up a gap, it is well known that the migration timescales are increased compared to a planet which has not been able to open up a gap, due to the action of these torques. For a disc with a greater level of self-gravity, it is expected that the turbulence due to this would act to close the gap. Therefore the gap properties are likely to be different for different values of the cooling. For faster cooling and therefore more gravitational stress and thus more turbulence, the gap is likely to close, causing the migration timescale to increase. Figure 8 shows the surface mass density profile of the discs once the planet has opened up a gap. The peak in the surface mass density at ≈ 100 AU is due to the circumplanetary disc while the density drop either side of the planet's orbital radius is due to the gap that has formed. It can be seen that the difference between the gap properties is not very distinct. The surface mass density outside the gap for $\beta = 15$ shows the only significant difference between the three simulations. Figure 9 shows the semi-major axis evolution over time for the three discs. It can be seen that migration acts much slower in these simulations than those presented in Section 5.1 since these planets have been allowed to open up a gap. However, the difference between the migration rate results for different levels of turbulence is somewhat unexpected since the migration rate for the disc with the largest amount of turbulence ($\beta = 15$) is lower than those for lower levels of turbulence. This result is currently being investigated.

6 Preliminary thoughts and future directions

We carry out two-dimensional simulations of a planet in a self-gravitating disc and consider the effects of varying the amount of turbulence due to the self-gravity on the migration of the planet. We find that if we do not allow the planet to open up a gap, the planet migrates rapidly regardless of the level of turbulence. On the other hand, if a gap is allowed to open up, the amount of self-gravity affects the subsequent migration rate in the disc.

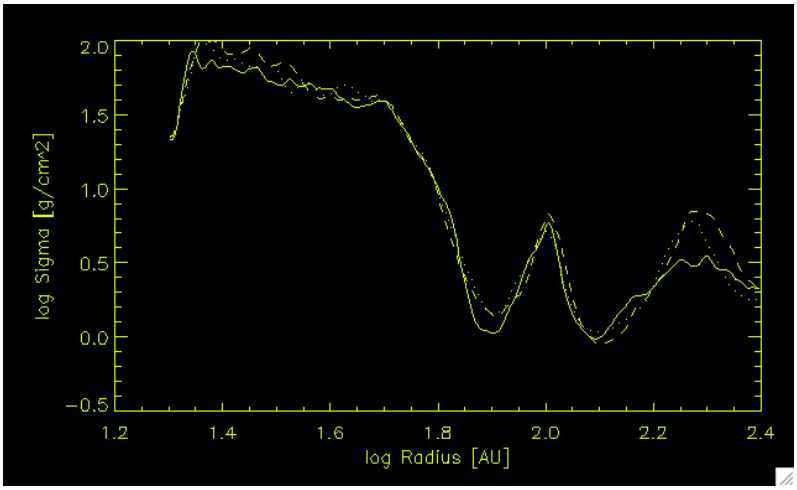

Figure 8: Surface mass density profile of the discs modelled with a cooling timescale, $\beta = 15$ (solid line), 20 (dotted line) and 30 (dashed line) at the end of the simulation. The circumplanetary disc causes a surface mass density peak at ≈ 100 AU and the gap can be identified by the density trough either side of the peak. The surface mass density profiles for each of the simulations are quite similar.

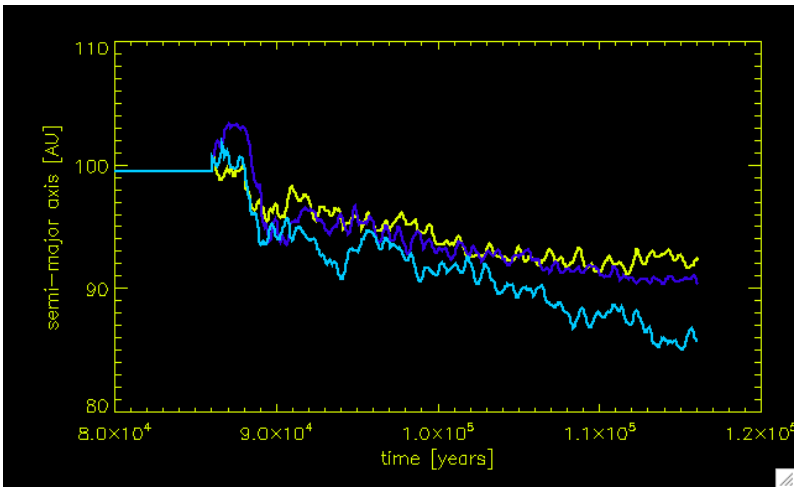

Figure 9: Plot of semi-major axis over time for the simulations which force the planet to open up a gap. The migration rate for the disc with a higher level of tubulence ($\beta = 15$; yellow line) is slower than that for the intermediate ($\beta = 20$; blue line) or low level of turbulence ($\beta = 30$; cyan line) which is somewhat unexpected.

In this project we have initially chosen to carry out low resolution simulations, to be able to produce initial results and form preliminary conclusions. However, higher resolution simulations are required to test for convergence. In addition, we would like to test these results with a laminar disc model using a set value of α to test if this approximation is valid since the link between the cooling timescale, β, and the gravitational stress, $\alpha_{\rm GI}$, expressed in equation 4 may not be so clear in the regime where a planet is introduced. In addition, in real discs, β is not constant over an entire disc and therefore, more realistic thermodynamics are required. Finally, we have set up a self-gravitating disc and introduced the planet at a later time. It would, however, be particularly interesting to be able to follow the formation and migration of the planet at the same time so that the evolution is self-consistently followed.

7 Acknowledgments

The simulations presented were run on the Grape cluster at University of California, Santa Cruz. We would like to thank Sijme-Jan Paardekooper and Andrew Youdin for useful discussions.

References

Baruteau, C. & Masset, F. 2008a, ApJ, 672, 1054

Baruteau, C. & Masset, F. 2008b, ApJ, 678, 483

Boss, A. P. 1997, Science, 276, 1836

Cameron, A. G. W. 1978, Moon and Planets, 18, 5

Fukagawa, M., Hayashi, M., Tamura, M., et al. 2004, ApJ, 605, L53

Gammie, C. F. 2001, ApJ, 553, 174

Goldreich, P. & Tremaine, S. 1979, ApJ, 233, 857

Goldreich, P. & Ward, W. R. 1973, ApJ, 183, 1051

Grady, C. A., Polomski, E. F., Henning, T., et al. 2001, AJ, 122, 3396

Harris, A. W. 1978, in Lunar and Planetary Inst. Technical Report, Vol. 9, Lunar and Planetary Institute Science Conference Abstracts, 459–461

Kalas, P., Graham, J. R., Chiang, E., et al. 2008, Science, 322, 1345

Kuiper, G. P. 1951, in 50th Anniversary of the Yerkes Observatory and Half a Century of Progress in Astrophysics, ed. J. A. Hynek, 357–+

Lafrenière, D., Jayawardhana, R., & van Kerkwijk, M. H. 2010, ApJ, 719, 497

Lagrange, A., Bonnefoy, M., Chauvin, G., et al. 2010, Science, 329, 57

Lodato, G. & Rice, W. K. M. 2004, MNRAS, 351, 630

Lodato, G. & Rice, W. K. M. 2005, MNRAS, 358, 1489

Marois, C., Macintosh, B., Barman, T., et al. 2008, Science, 322, 1348

Masset, F. 2000, AAPS, 141, 165

Matzner, C. D. & Levin, Y. 2005, ApJ, 628, 817

Meru, F. & Bate, M. R. 2010, MNRAS, 1504

Mizuno, H. 1980, Progress of Theoretical Physics, 64, 544

Perri, F. & Cameron, A. G. W. 1974, Icarus, 22, 416

Rafikov, R. R. 2005, ApJ, 621, L69

Rice, W. K. M., Lodato, G., & Armitage, P. J. 2005, MNRAS, 364, L56

Safronov, V. S. 1969, Evoliutsiia doplanetnogo oblaka. (Nakua, Moscow)

Toomre, A. 1964, ApJ, 139, 1217

Ward, W. R. 1991, in Lunar and Planetary Institute Science Conference Abstracts, Vol. 22, Lunar and Planetary Institute Science Conference Abstracts, 1463–+